Thermodynamic Measurements on *n*-Hexadecane ($C_{16}H_{34}$) and *n*-Heptadecane ($C_{17}H_{36}$) at Elevated Pressures

A. Würflinger and M. Sandmann

Lehrstuhl für Physikalische Chemie II, Ruhr-Universität, D-44780 Bochum

Reprint requests to Prof. A. W.; Albert.Wuerflinger@ruhr-uni-bochum.de

Z. Naturforsch. **55a,** 533–538 (2000); received February 16, 2000

Specific volumes of *n*-hexadecane (*n*-$C_{16}H_{34}$) and *n*-heptadecane (*n*-$C_{17}H_{36}$) are presented for temperatures between 298 and 348 K and pressures up to 280 MPa. The melting curve for *n*-$C_{16}H_{34}$ was determined with differential thermal analysis. The *pVT* data are established for the liquid, solid and (in the case of *n*-$C_{17}H_{36}$) rotator phases. For *n*-$C_{16}H_{34}$ the density immediately below the freezing temperature is larger than for *n*-$C_{17}H_{36}$ immediately below the rotational transition temperature. Changes of volume, enthalpy, and entropy along the phase transitions are reported. The volume change of melting decreases distinctly with increasing pressure, whereas the volume change at the rotational transition is much less pressure-dependent. Enthalpy and entropy changes have been calculated with the aid of the Clausius-Clapeyron equation.

Key words: Hexadecane, Heptadecane; DTA; *pVT*, High Pressure; Phase Transitions.

1. Introduction

DTA (Differential thermal analysis) and *pVT* measurements have been performed for many plastic crystals in the last years [1, 2]. In the present contribution we present results for some *n*-alkanes, which play an important role as model systems for lipids, polymers and liquid crystals [3, 4]. In particular multi-component systems of *n*-alkanes are used as thermal protection materials and for energy storage applications, and therefore their excess thermodynamic properties of the rotator phase solid solutions have been analysed in detail [5, 6]. Whereas densities of the liquid state for *n*-alkanes have been reported by many authors [7, 8], only few pressure-volume studies are concerned with the solid state [9–12]. *pVT* data of *n*-alkanes have been widely used to model the equation of state [13] which enables also to calculate the volume-dependent part of the entropy of melting [14]. We studied *n*-$C_{16}H_{34}$ ($M = 226.44$ g/mol) and *n*-$C_{17}H_{36}$ ($M = 240.47$ g/mol) in the neighbourhood of their phase transitions (crystal → rotator phase → liquid) up to 300 MPa. Volume and enthalpy changes accompanying the phase transitions are reported.

2. Experimental

2.1. Differential Thermal Analysis

The high-pressure equipment for the DTA measurements has been described in [15]. Samples (~ 50 mg) of *n*-$C_{16}H_{34}$ are enclosed in small containers made of indium. DTA thermograms are recorded using heating rates of 1 ~ 2 K min^{-1} at constant pressures. For *n*-$C_{17}H_{36}$ results from previous DTA measurements are available [16].

2.2. PVT Measurements

The densities at atmospheric pressure were determined with a vibrating-tube density meter Anton Paar DMA58. The high-pressure dilatometric cell is described in [2, 17]. The sample is separated from the pressurizing gas by a moving piston whose displacement is recorded inductively. The measurements are performed at constant temperature on releasing the pressure step by step. The recorded raw volume data are refined with a computer program (corrections for the hysteresis pressure, expansivity and compressibility of the dilatometric cell etc.) and then combined with the specific volumes determined at atmospheric pressure. Thus specific volume data are established for higher pressures.

2.3. Materials

The alkanes were purchased from Acros (purity 99%) and used without further purification.

3. Results and Discussion

3.1. Phase Diagrams

The melting curve of hexadecane was established with DTA and is presented in Figure 1. There is excellent

0932-0784 / 00 / 0500-0533 $ 06.00 © Verlag der Zeitschrift für Naturforschung, Tübingen · www.znaturforsch.com

Table 1. Specific volumes ($cm^3 \cdot g^{-1}$) for n-$C_{16}H_{34}$.

p/MPa	T/K					
	298.15	303.15	313.15	323.15	333.15	343.15
0.1	1.2982	1.3041	1.3160	1.3281	1.3405	1.3531
10	1.285	1.292	1.303	1.317	1.327	1.339
20	1.273	1.280	1.292	1.305	1.315	1.327
30	1.077	1.270	1.281	1.295	1.304	1.315
40	1.074	1.262	1.271	1.285	1.294	1.304
50	1.071	1.254	1.262	1.276	1.284	1.294
60	1.067	1.071	1.253	1.267	1.275	1.285
70	1.064	1.068	1.246	1.258	1.267	1.276
80	1.061	1.065	1.239	1.250	1.259	1.268
90	1.058	1.062	1.233	1.243	1.252	1.260
100	1.056	1.059	1.068	1.236	1.245	1.253
110	1.053	1.057	1.064	1.230	1.239	1.246
120	1.050	1.054	1.061	1.225	1.233	1.239
130	1.048	1.052	1.058	1.219	1.227	1.233
140	1.046	1.049	1.055	1.215	1.222	1.228
150	1.043	1.047	1.052	1.065	1.217	1.222
160	1.041	1.045	1.050	1.061	1.212	1.217
170	1.039	1.043	1.047	1.057	1.207	1.212
180	1.037	1.041	1.045	1.054	1.202	1.208
190	1.035	1.039	1.043	1.051	1.197	1.203
200	1.034	1.038	1.041	1.048	1.068	1.199
210	1.032	1.036	1.039	1.046	1.061	1.195
220	1.031	1.034	1.037	1.044	1.056	1.190
230	1.029	1.033	1.036	1.041	1.051	1.186
240	1.028	1.032	1.035	1.040	1.047	1.182
250	1.027	1.030	1.034	1.038	1.043	1.177
260	1.026	1.029	1.033	1.037	1.041	1.065
270	1.025	1.028	1.032	1.035	1.039	1.052
280	1.024	1.027	1.031	1.034	1.038	1.045

Table 2. Specific volumes ($cm^3 \cdot g^{-1}$) for n-$C_{17}H_{36}$.

p/MPa	T/K					
	303.15	313.15	323.15	333.15	343.15	348.15
0.1	1.2963	1.3079	1.3196	1.3317	1.3439	1.3501
10	1.284	1.296	1.308	1.319	1.331	1.337
20	1.273	1.285	1.297	1.309	1.319	1.325
30	1.263	1.274	1.287	1.299	1.308	1.314
40	1.139	1.264	1.277	1.289	1.297	1.303
50	1.131	1.255	1.268	1.280	1.287	1.293
60	1.123	1.246	1.259	1.271	1.278	1.283
70	1.115	1.238	1.251	1.263	1.269	1.275
80	1.073	1.231	1.243	1.255	1.261	1.266
90	1.069	1.127	1.236	1.247	1.253	1.258
100	1.066	1.120	1.229	1.240	1.246	1.251
110	1.063	1.112	1.223	1.233	1.239	1.244
120	1.061	1.105	1.217	1.226	1.233	1.237
130	1.058	1.064	1.212	1.220	1.227	1.231
140	1.055	1.061	1.207	1.214	1.221	1.225
150	1.053	1.058	1.119	1.208	1.215	1.219
160	1.050	1.056	1.107	1.203	1.210	1.214
170	1.048	1.053	1.063	1.199	1.205	1.209
180	1.046	1.051	1.060	1.194	1.201	1.204
190	1.043	1.048	1.058	1.190	1.196	1.200
200	1.041	1.046	1.055	1.078	1.191	1.195
210	1.040	1.044	1.052	1.071	1.187	1.191
220	1.038	1.042	1.050	1.064	1.183	1.187
230	1.036	1.040	1.047	1.059	1.178	1.183
240	1.034	1.038	1.045	1.054	1.174	1.179
250	1.033	1.036	1.043	1.051	1.169	1.176
260	1.031	1.035	1.041	1.048	1.165	1.172
270	1.030	1.033	1.039	1.046	1.066	1.168
280	1.029	1.032	1.038	1.045	1.060	1.164

agreement with data from Tanaka et al. [18] who determined the phase transition by a visual observation; therefore the DTA data were used to fit the melting curve. Dymond et al. [19] determined freezing pressures in p, ϱ, T measurements resulting in a phase boundary lying below the DTA melting curve. That is, the freezing temperatures are shifted to higher pressures at a given temperature. The same behaviour (although to a less extent) was observed in the p, V, T measurements of the present work.

In the case of heptadecane (Fig. 2) the DTA transition points are taken from [16]. Data from p, V, T measurements are included in Fig. 2, showing again the shift to higher pressures. In the volume measurements the transition close to the triple point (crystal – rotator phase – liquid) at 240 MPa and 340 K [16] were not well separated. Therefore a combined set of DTA points [16] and pVT points of the present study were used for fitting the transition lines of n-$C_{17}H_{36}$. The following polynomials of second order represent the $T(p)$ phase transition lines:

n-$C_{16}H_{34}$:	melting:	Cr → L	$T/K = 291.2 + 0.2411\ (p/MPa) - 1.4938 \cdot 10^{-4}\ (p/MPa)^2$
n-$C_{17}H_{36}$:	melting:	R → L	$T/K = 294.7 + 0.2347\ (p/MPa) - 1.8784 \cdot 10^{-4}\ (p/MPa)^2$
		Cr → L	$T/K = 286.2 + 0.2836\ (p/MPa) - 2.4552 \cdot 10^{-4}\ (p/MPa)^2$
	rot. tr.:	Cr → R	$T/K = 284.6 + 0.2619\ (p/MPa) - 1.2497 \cdot 10^{-4}\ (p/MPa)^2$

3.2. *p,V,T Measurements*

In Fig. 3 and 4 the $v(p)$-isotherms are plotted for various temperatures. Volume changes accompanying the phase transitions (Cr → L, Cr → R, R → L) are clearly discerned as steps in the isotherms. Other high-pressure volume data are only available for the liquid state of n-$C_{16}H_{34}$ [19–23] and n-$C_{17}H_{36}$ [24, 25]. Figure 3 shows one isotherm (348 K [19]) for comparison. For each phase the $v(p)$ isotherms have been fitted to polynomials, from which the specific volumes are calculated in

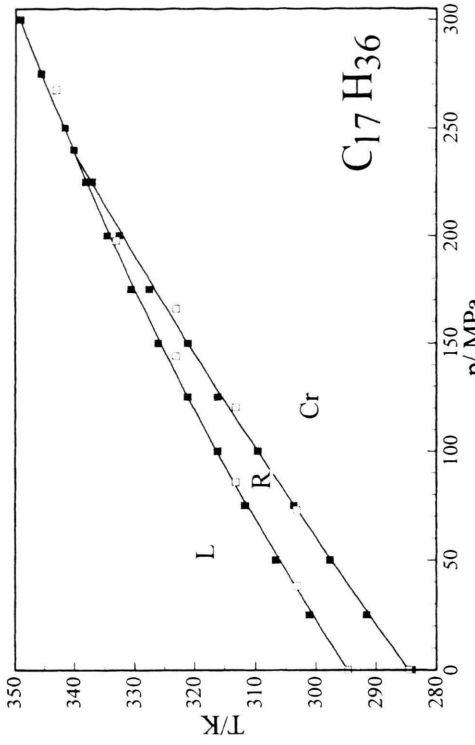

Fig. 2. Phase diagram of *n*-heptadecane, ■ : DTA [16], □ : pVT, this work.

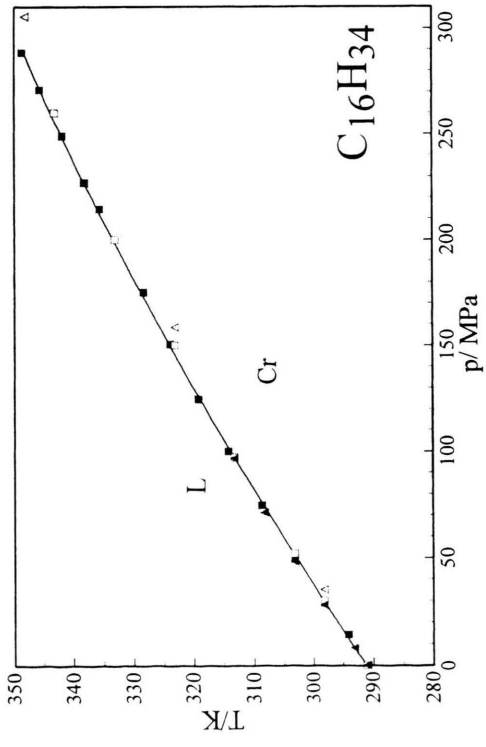

Fig. 1. Melting curve of *n*-hexadecane, ■ : DTA, this work, □ : pVT, this work, ▲ : [18], △ : [19].

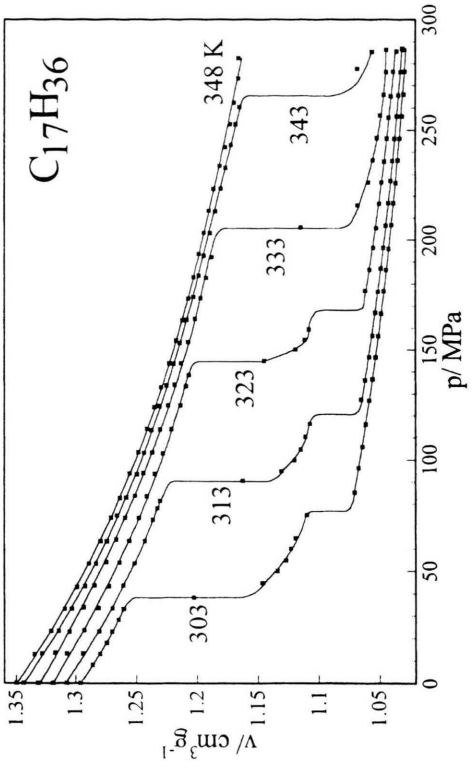

Fig. 4. Specific volumes for *n*-heptadecane as a function of pressure.

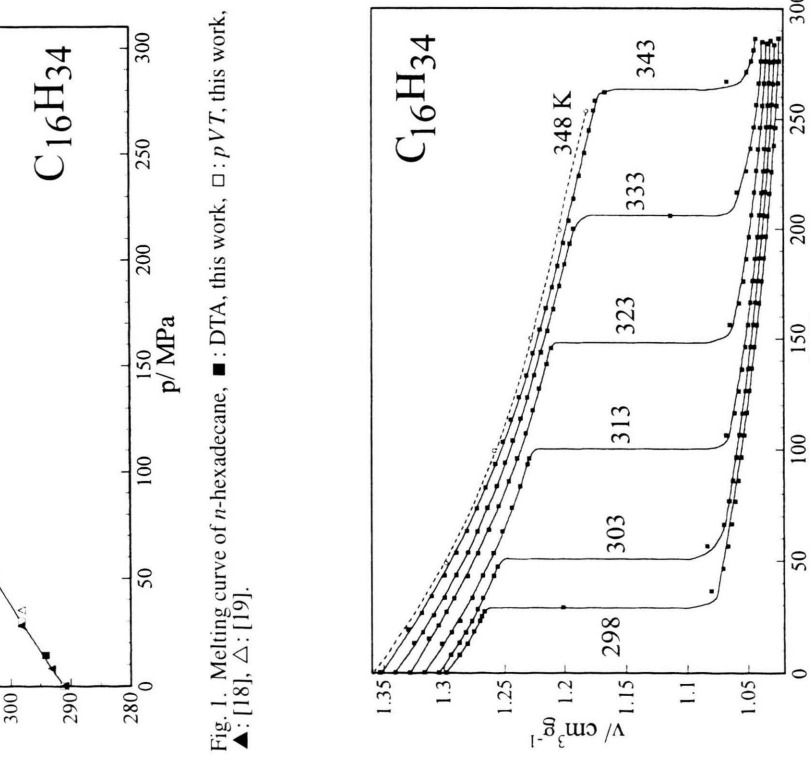

Fig. 3. Specific volumes for *n*-hexadecane as a function of pressure, — this work, · · · [19].

Table 3. Specific volumes ($cm^3 \cdot g^{-1}$) for the liquid state in comparison with literature data.

$C_{16}H_{34}$				$C_{17}H_{36}$			
p/MPa	*T*/K	This work	Literature data	*p*/MPa	*T*/K	This work	Literature data
0.1	291.15*	1.2900	1.2901 [14]	0.1	294.7*	1.2866	1.2879 [14]
	298.15	1.2982	1.2984 [19]		298.15	1.2906	1.2912 [29]
			1.2971 [26]				1.2912 [30]
	303.15	1.3041	1.3059 [26]		303.15	1.2963	1.2968 [31]
	313.15	1.3160	1.3162 [26]				1.2958 [24]
			1.3162 [27]		313.15	1.3079	1.3076 [24]
	323.15	1.3281	1.3280 [28]		323.15	1.3196	1.3195 [24]
	333.15	1.3405	1.3406 [28]				1.3194 [32]
			1.3401 [23]		333.15	1.3317	1.3316 [24]
	343.15	1.3531	1.3533 [28]		343.15	1.3439	1.3439 [24]
10	323.15	1.317	1.3164 [28]	100	323.15	1.229	1.2343 [25]
	333.15	1.327	1.3278 [28]				1.2230 [24]
			1.3261 [23]		333.15	1.240	1.2404 [24]
	343.15	1.339	1.3395 [28]		343.15	1.246	1.2478 [24]
30	333.15	1.304	1.3023 [23]	200	343.15	1.191	1.1949 [24]
120	323.15	1.225	1.2277 [19]				

* melting point.

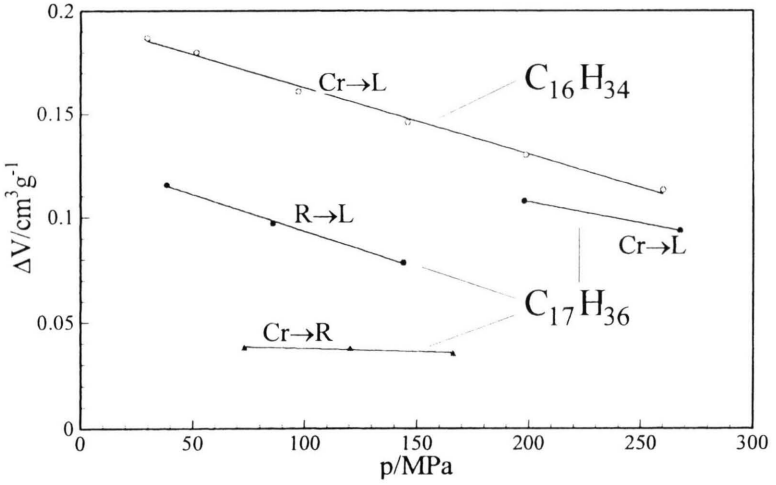

Fig. 5. Volume changes at the phase transitions for n-$C_{16}H_{34}$ and n-$C_{17}H_{36}$.

Table 4. Thermodynamic properties of n-hexadecane and n-heptadecane.

n-alkane	Transition	*T*/K	*p*/MPa	ΔV_m/ $cm^3 \cdot mol^{-1}$	ΔH_m/ $kJ \cdot mol^{-1}$	ΔS_m/ $J \cdot mol^{-1} \cdot K^{-1}$
$C_{16}H_{34}$	Cr → L	291.15	0.1	44.15	53.3	183
		298.15	30	42.37	54.5	182
		303.15	52	40.70	54.7	180
		313.15	97	36.29	53.8	172
		323.15	150	33.11	54.5	169
		333.15	200	29.47	54.1	163
		343.15	260	25.49	53.5	156
$C_{17}H_{36}$	R → L	294.7	0.1	30.82	38.6	131
		303.15	38.2	27.62	38.0	125
		313.15	85.7	23.63	36.5	117
		323.15	143.9	18.75	33.5	104
	Cr → R	284.65	0.1	9.77	10.6	37.3
		303.15	72.9	9.24	11.5	37.9
		313.15	120.3	8.89	12.0	38.3
		323.15	166.0	8.55	12.5	38.8
	Cr → L	333.15	197.7	16.32/9.58	33.9/15.0	102/45
		343.15	267.6	22.5	50.8	148

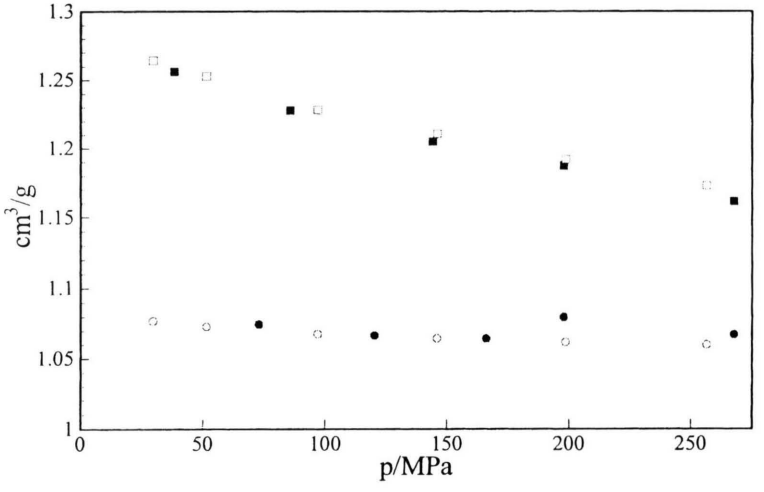

Fig. 6. Specific volumes along the phase transitions, n-$C_{16}H_{34}$: □ Liquid, ○ crystal, n-$C_{17}H_{36}$: ■ Liquid, ● crystal.

steps of 10 MPa, they are listed in the Tables 1 and 2; a solid line in a column separates different phases. The specific volumes in the first line (0.1 MPa) (obtained with the vibrating-tube density meter) have a higher accuracy ($\sim 10^{-4}$) than the high-pressure data ($\sim 10^{-3}$). In Table 3, specific volumes for the liquid state are compared with literature data. The values at the melting point at 0.1 MPa have been obtained by extrapolation from higher temperatures. The agreement with the atmospheric pressure data is satisfactory. Regarding the pressure dependence, we find a somewhat larger decrease of the specific volumes with increasing pressure than reported in [20, 21, 25].

In Fig. 5 the volume changes accompanying the phase transitions are displayed. The ΔV values have been obtained by extrapolating the fitted $v(p)$ isotherms to the transition point. Figure 4 shows that the transition R → L is not sharp, rendering an unambiguous estimation of $\Delta V_{R\to L}$ rather difficult. The melting exhibits a certain pretransition effect as well, that was also noted by Ter Minassian et al. for $C_{16}H_{34}$ [33], and by Scaife et al. for $C_{15}H_{32}$ [34]. For the evaluation of the ΔV values the pretransition region was included. Clearly, ΔV of melting decreases with increasing pressure, whereas it remains fairly constant for the transition to the rotator phase. Some results are collected in Table 4, where ΔH values have been calculated with the aid of the Clausius-Clapeyron equation. The transition pressures in Table 4 are taken from the volume measurements. The state point at 197.7 MPa is below the triple point, and therefore the observed volume change was splitted into two contributions for the rotational transition and melting, respectively, assuming a ratio $\Delta V_{R\to L}: \Delta V_{Cr\to R} = 63:37$. This ratio was estimated by extrapolating the pressure dependence from the state points at lower pressures.

The pressure dependence of ΔH is less pronounced than that of ΔV. In case of the rotational transition, ΔH even increases a little bit with increasing pressure. This feature has also been observed for other odd *n*-alkanes [9, 12]. Extrapolation to atmospheric pressure yields: *n*-$C_{16}H_{34}$: $\Delta V_{Cr\to L} = 44.2$ cm^3/mol (45.7 [35]), $\Delta H_{Cr\to L} = 53.3$ kJ/mol (53 [36]), *n*-$C_{17}H_{36}$: $\Delta V_{R\to L} = 30.8$ cm^3/mol (29.4 [11]), $\Delta H_{R\to L} = 38.6$ kJ/mol (39.4 [36]), $\Delta V_{Cr\to R} = 9.77$ cm^3/mol, $\Delta H_{Cr\to R} = 10.6$ kJ/mol (10.8 [36]). Literature values in parentheses are shown for comparison.

In Fig. 6 we compare the specific volumes along the melting and at the Cr → R transition. In the liquid state *n*-$C_{16}H_{34}$ has a larger specific volume than *n*-$C_{17}H_{36}$, and vice versa in the Cr phase. This result is in agreement with previous findings, showing that the even *n*-alkanes are more closely packed than the odd ones [10, 12, 37]. Extrapolation to atmospheric pressure results in v (liquid) $= 1.280$ cm^3 g^{-1}, v (crystal) $= 1.081$ cm^3 g^{-1} for *n*-$C_{16}H_{34}$, and v (liquid) $= 1.275$ cm^3 g^{-1}, v (crystal) $= 1.082$ cm^3 g^{-1} for *n*-$C_{17}H_{36}$. The v (liquid) values extrapolated from high pressures, do not agree with the atmospheric pressure data extrapolated to the melting point (see Table 3). This might be due to the insufficient number of experimental points along the phase boundary that does not enable a proper extrapolation to 1 atm, all the more the *n*-alkanes exhibit a relatively large compressibility in the low-pressure region. On the other hand, the densities of the solid phases can be estimated from crystallographic data: *n*-$C_{16}H_{34}$ [38]: triclinic, $Z=1$, $V=406$ Å^3 ⇒ $v = 1.080$ cm^3 g^{-1}; *n*-$C_{17}H_{36}$ [39]: orthorhombic, $Z=4$, $V=1750$ Å^3 ⇒ $v = 1.096$ cm^3 g^{-1}, see also [40]. For *n*-$C_{16}H_{34}$ there is good agreement with v (crystal), but not for *n*-$C_{17}H_{36}$. It can be recognized from Fig. 6 that in the case of *n*-$C_{16}H_{34}$ there are many more points in the low-pressure region allowing a better extrapolation than for *n*-$C_{17}H_{36}$, for which v (crystal) data are particularly scattered around the triple point. For future investigations it is recommended to perform more measurements in the low-pressure region in smaller steps of pressures and temperatures in order to achieve a reliable extrapolation and comparison with atmospheric pressure data.

Acknowledgement

Grants from the Fonds der Chemischen Industrie are gratefully acknowledged. A. W. thanks Dr. M. Jenau for some technical advices and Dr. D. Mondieig for helpful discussions.

[1] M. Jenau, M. Sandmann, A. Würflinger, and J. Ll. Tamarit, Z. Naturforsch. **52a,** 493 (1997).
[2] M. Jenau and A. Würflinger, Z. Physik. Chem. Frankfurt **199,** 255 (1997); F. Hamann and A. Würflinger, Z. Physik. Chem. **211,** 85 (1999).
[3] S. P. Srivastava, J. Handoo, K. M. Agrawal, and G. C. Joshi, J. Phys. Chem. Solids **54,** 639 (1993).
[4] E. B. Sirota and D. M. Singer, J. Chem. Phys. **101,** 10873 (1994).
[5] D. Mondieig, P. Espeau, L. Roblès, Y. Haget, H. A. J. Oonk, and M. A. Cuevas-Diarte, J. Chem. Soc. Faraday Trans. **93,** 3343 (1997).
[6] H. A. J. Oonk, D. Mondieig, Y. Haget, and M. A. Cuevas-Diarte, J. Chem. Phys. **108,** 715 (1998).
[7] I. Cibulka and L. Hnedkovsky, J. Chem. Eng. Data **41,** 657 (1996); I. Cibulka and T. Takagi, J. Chem. Eng. Data **44,** 1105 (1999).

[8] M. M. Aalto and K. I. Keskinen, Fluid Phase Equil. **166,** 183 (1999).
[9] R. R. Nelson, W. Webb, and J. A. Dixon, J. Chem. Phys. **33,** 1756 (1960).
[10] W. Dollhopf, H. P. Grossmann, and U. Leute, Coll. & Polym. Sci. **259,** 267 (1981).
[11] A. Turturro and U. Bianchi, J. Chem. Phys. **62,** 1668 (1975).
[12] R. Landau and A. Würflinger, Ber. Bunsenges. Phys. Chem. **84,** 895 (1980).
[13] R. Simha and U. Yahsi, Faraday Trans. **91,** 2443 (1995); R. K. Jain and R. Simha, J. Chem. Phys. **70,** 5329 (1979); Ber. Bunsenges. Phys. Chem. **85,** 626 (1981).
[14] A. Würflinger, Colloid Polymer Sci. **262,** 115 (1984).
[15] A. Würflinger, Ber. Bunsenges. Phys. Chem. **79,** 1195 (1975); N. Pingel, U. Poser, and A. Würflinger, J. Chem. Soc. Faraday Trans. I **80,** 3221 (1984).
[16] A. Würflinger and G. M. Schneider, Ber. Bunsenges. Phys. Chem. **77,** 121 (1973).
[17] R. Landau and A. Würflinger, Rev. Sci. Instrum. **51,** 533 (1980).
[18] Y. Tanaka and M. Kawakami, Fluid Phase Equil. **125,** 103 (1996).
[19] J. H. Dymond, K. J. Young, and J. D. Isdale, J. Chem. Thermodyn. **11,** 887 (1979).
[20] J.W. M. Boelhouwer, Physica **26,** 1021 (1960).
[21] R. G. Snyder and J. Winnick, Proc. Symp. Thermoph. Prop. 5th. (1970) 115. CA: 76 28467a.
[22] M. Glaser, C. J. Peters, H. J. van der Kooi, and R. N. Lichtenthaler, J. Chem. Thermodyn. **17,** 803 (1985).
[23] J.-Sheng Chang, Ming-Jer Lee, and Ho-mu Lin, J. Chem. Eng. Data **43,** 233 (1998).
[24] W. Brostow, T. Grindley, and A. Macip, Mater. Chem. Phys. **12,** 37 (1985).
[25] A. K. Doolittle, J. Chem. Eng. Data **9,** 275 (1964).
[26] M. M. El-Banna and M. M. El-Batouti, Can. J. Chem. **76,** 1860 (1998).
[27] G. Hahn and P. Svejda, J. Chem. Eng. Data **41,** 619 (1996); G. Hahn, K. Ulcay, P. Svejda, and M. A. Siddiqi, J. Chem. Eng. Data **41,** 319 (1996).
[28] T. S. Banipal, S. K. Garg, and J. C. Ahluwalia, J. Chem. Thermodyn. **23,** 923 (1991).
[29] M. D. Peña and C. Menduiña, J. Chem. Thermodyn. **6,** 387 (1974).
[30] F. D. Rossini, Selected values in: Amer. Petrol. Inst. Res. Proj. 44, 288 (1953); USA.
[31] A. Audsley and F. R. Goss, J. Chem. Soc. **9,** 2989 (1950).
[32] D. V. S. Jain and V. K. Gombar, J. Chem. Soc. Faraday Trans. 1, **75,** 1132 (1979).
[33] L. Ter Minassian and P. Pruzan, J. Chem. Thermodyn. **9,** 375 (1977).
[34] W. G. S. Scaife and C. G. R. Lyons, J. Chem. Thermodyn. **17,** 623 (1985).
[35] A. van Hook and L. Silver, J. Chem. Phys. **10,** 686 (1942).
[36] P. Espeau, L. Roblès, D. Mondieig, Y. Haget, M. A. Cuevas-Diarte, and H. A. J. Oonk, J. Chim. Phys. **93,** 1217 (1996).
[37] W. F. Seyer, R. F. Patterson, and J. L. Keays, J. Amer. Chem. Soc. **66,** 179 (1944).
[38] N. Norman and H. Mathisen, Acta Chem. Scand. **26,** 3913 (1972).
[39] J. Doucet, I. Denicolo, and A. F. Craievich, J. Chem. Phys. **75,** 1523 (1981).
[40] S. R. Craig, G. P. Hastie, K. J. Roberts, and J. N. Sherwood, J. Mater. Chem. **4,** 977 (1994).